2013 European Control Conference (ECC)
July 17-19, 2013, Zürich, Switzerland.

A novel leader-following strategy applied to formations of quadrotors

Valter Roldão, Rita Cunha, David Cabecinhas, Carlos Silvestre, and Paulo Oliveira

Abstract— **This paper presents a strategy for formation control of autonomous vehicles using a leader-following approach. A trajectory planner prescribes the motion of a group of virtual vehicles, using a Lyapunov-based nonlinear controller that stabilizes the position of the leader in the reference frame of the virtual vehicles at a predefined distance vector. This strategy differs from the standard approach of defining the desired distance vector in an inertial frame and can be used to obtain rich formation trajectories with varying curvatures between vehicles. By imposing adequate constraints on the motion of the virtual vehicles, the planner naturally guarantees the generation of valid formation trajectories, without requiring the parametrization of the space curve described by the leader. The trajectories are generated online and provided to a trajectory tracking controller specifically designed for quadrotor vehicles. Results of experimental tests are presented demonstrating the performance of the proposed solution for formation control of autonomous vehicles.**

I. Introduction

The problem of cooperative control of multi-vehicle systems poses an important challenge to automatic control. It has been the scope of a number of publications and experimental results are beginning to appear [1]–[7]. Multi-vehicle systems have proven to be advantageous in carrying out a variety of tasks such as surveillance and area exploration [2], where it results in a faster and more efficient process, or load transportations [3], where the employment of multiple robots allows for the use of smaller vehicles.

Within the field of cooperative control, the problem of maintaining a multi-vehicle formation while moving in space, known as formation control, has received considerable attention, with several methodologies proposed over the past 15 years. Most of them employ the concept of artificial potentials to control the robot constellation. One such example is the work developed by Leonard and Fiorelli [4], where they proposed the use of potential fields associated with moving reference points, which they called *virtual leaders*, whose function was to shape and give reference movement to the formation. With this strategy it is possible to control the shape and orientation of the formation by proper positioning of the virtual leaders, although generating their trajectories may be difficult. Other approaches making use of artificial potentials may be found in [5] and [6]. However, these later strategies do not enforce a definite vehicle configuration, only driving the vehicles to fixed distances relative to each other.

In the method for vehicle formation presented in this paper, a trajectory planner prescribes the motion of a group of virtual vehicles so as to follow a leader and a trajectory tracking controller uses the generated trajectories as references for real vehicles. The trajectory planner is in fact a nonlinear control law that stabilizes, at a predefined distance vector, the position of the leader in the body frame of the virtual follower. This strategy differs from the majority of approaches found in the literature, which define the desired distance vector in either the body frame of the leader (see [8], for an example applied to unicycles) or the inertial frame (see [9], for an example applied to quadrotors). Notice that the latter can only be used to define formations where the followers describe an offset version of the leader's trajectory. In contrast, the current approach can be used to generate richer formation trajectories, in the sense that the followers can describe trajectories that differ considerably from that of the leader, namely in terms of curvature. Moreover, these and other path parameters do not need to be explicitly computed from the leader's path.

The solution proposed exhibits some additional properties of interest. Given that the leader-follower distance is expressed in the body frame of the follower, relative position measurements can be directly acquired by sensors installed on-board the follower vehicles. Also, the trajectories are generated at runtime, based solely on the motion of the leader, which is tracking a preassigned trajectory unknown to the followers. As such, deviations in the leader's motion are captured by the planner and the trajectories to be tracked are changed accordingly.

The adopted approach of defining the position error in the body frame of the follower dictates the existence of an internal dynamics given by the angular distance between vehicles, whose boundedness must be guaranteed in order to generate valid formation trajectories. Such result is ensured by imposing adequate constraints on the motion of the virtual vehicles and guaranteeing that well-defined conditions relating the curvature of the leader's trajectory and the desired distance between vehicles are satisfied, so that stabilizing the position of the leader in the body frame of the virtual follower naturally entails an attitude stabilization.

This paper is structured as follows. Section II describes the trajectory planner and presents simulation results for the generation of reference follower trajectories. Section III focuses on the experimental part of the work. The testbed used for the experiments is described and the results of a test where two quadrotors follow a third one describing a formation trajectory around a lemniscate are presented and discussed. Finally, section IV summarizes the contents of the paper.

II. Leader-follower trajectory generation

Consider a two-dimensional world where a group of vehicles tries to follow a leader whose motion at each time instant t is known up to the second derivative $\{\mathbf{p}_L(t), \dot{\mathbf{p}}_L(t), \ddot{\mathbf{p}}_L(t)\}$. The objective of the vehicles is to move in such a way as to *see* the leader always in the same relative position. Each follower moves independently of its peers. Thus, for most of the coming description a generic follower is used.

This work was partly funded by Fundação para a Ciência e Tecnologia (FCT) under the Projects PEst-OE/EEI/LA0009/2011 and SCARVE-PTDC/EEA-CRO/102857/2008.

The authors are with the Department of Electrical Engineering and Computer Science, and Institute for Systems and Robotics, Instituto Superior Técnico, 1046-001 Lisbon, Portugal. Carlos Silvestre is with the Faculty of Science and Technology, University of Macau, Taipa, Macau.

A. Problem Formulation

The goal of the trajectory planner is to define a control law for the virtual follower that drives the position of the leader relative to the follower to a desired distance vector. Let $\{I\}$ denote the inertial reference frame, $\{L\}$ the body frame of the leader, and $\{F\}$ the body frame of the follower. The configuration of $\{F\}$ with respect to $\{I\}$, can be expressed using an element of the Special Euclidean Group, $(\mathcal{R}, \mathbf{p}_F) = \left({}^I_F\mathbf{R}, {}^I\mathbf{p}_F\right) \in SE(2)$. The rotation matrix $\mathcal{R}$ can be parametrized by an angle θ, representing the angular displacement between the two frames, so that,

$$\mathcal{R} = \begin{bmatrix} \cos\theta & -\sin\theta \\ \sin\theta & \cos\theta \end{bmatrix} \tag{1}$$

Using this notation, the position of leader relative to the follower can be written as

$${}^F\mathbf{p}_L = \mathcal{R}^T \left(\mathbf{p}_L - \mathbf{p}_F\right) \tag{2}$$

and the trajectory generation problem can be defined as the problem of designing a control law for the virtual follower that drives ${}^F\mathbf{p}_L$ to a desired distance vector

$$\mathbf{d} = [d_x \ d_y]^T \in \mathbb{R}^2.$$

To guarantee that the trajectory generation problem is well-defined, we introduce constraints on the motion of the virtual followers. These are actuated in terms of forward and angular accelerations so as to constrain their motion to the longitudinal direction.

The kinematic equations of motion can written as

$$\dot{\mathcal{R}} = \mathcal{R}\mathbf{S}\left(\omega\right) \tag{3}$$

$$\dot{\mathbf{p}}_F = \mathcal{R}\mathbf{i}u \tag{4}$$

where $u \in \mathbb{R}$ and $\omega \in \mathbb{R}$ are respectively the linear and angular speeds, $\mathbf{i} = [1 \ 0]^T$, and $\mathbf{S}\left(\omega\right)$ is a skew-symmetric matrix given by $\mathbf{S}\left(\omega\right) = \begin{bmatrix} 0 & -\omega \\ \omega & 0 \end{bmatrix}$.

The derivatives of the angular and linear speeds constitute the actuation and are given by

$$\dot{u} = T \tag{5}$$

$$\dot{\omega} = \tau \tag{6}$$

B. Controller Design

Let the position error be defined as

$$\mathbf{e}_1 = {}^F\mathbf{p}_L - \mathbf{d} \tag{7}$$

and consider the candidate Lyapunov function given by

$$V_1 = \frac{1}{2}\mathbf{e}_1^T\mathbf{e}_1. \tag{8}$$

Computing the time derivative of V_1 yields

$$\begin{aligned} \dot{V}_1 &= \mathbf{e}_1^T\left[-\mathbf{S}(\omega){}^F\mathbf{p}_L + \mathcal{R}^T\dot{\mathbf{p}}_L - u\mathbf{i}\right] \\ &= \mathbf{e}_1^T\left[-\mathbf{S}(\omega)\mathbf{d} + \mathcal{R}^T\dot{\mathbf{p}}_L - u\mathbf{i}\right] \\ &= -k_1{\mathbf{e_1}}^T\boldsymbol{\sigma}(\mathbf{e_1}) \\ &\quad + k_1{\mathbf{e_1}}^T\left[\boldsymbol{\sigma}(\mathbf{e_1}) + \frac{1}{k_1}\left(-\mathbf{S}(\omega)\mathbf{d} + \mathcal{R}^T\dot{\mathbf{p}}_L - u\mathbf{i}\right)\right] \end{aligned} \tag{9}$$

where the property that $\mathbf{e}_1^T\mathbf{S}(\omega)\mathbf{e}_1 = 0$ was used.

The term $\boldsymbol{\sigma}(.)$ is a sigmoidal saturation function, applied element wise, which is introduced to limit the influence of the position error on the actuation and is given by

$$\boldsymbol{\sigma}(\mathbf{e_1}) = p_{\max}\tanh\left(\mathbf{x}/p_{\max}\right) \tag{10}$$

where $p_{\max}$ is a configurable parameter.

Following the backstepping procedure, a new error is created and the Lyapunov candidate function extended to include it, so that

$$\mathbf{e}_2 = \boldsymbol{\sigma}(\mathbf{e_1}) + \frac{1}{k_1}\left(-\mathbf{S}(\omega)\mathbf{d} + \mathcal{R}^T\dot{\mathbf{p}}_L - u\mathbf{i}\right) \tag{11}$$

$$V_2 = \frac{1}{2}\sum_{i=1}^{2}{\mathbf{e_i}}^T\mathbf{e_i} \tag{12}$$

Defining

$$\boldsymbol{\Gamma} = \begin{bmatrix} 1 & -d_y \\ 0 & d_x \end{bmatrix} \tag{13}$$

$$\boldsymbol{\mu} = \begin{bmatrix} T \\ \tau \end{bmatrix} \tag{14}$$

$$\boldsymbol{\delta} = -\mathbf{S}(\omega)\mathcal{R}^T\dot{\mathbf{p}}_L + \mathcal{R}^T\ddot{\mathbf{p}}_L \tag{15}$$

$\dot{V}_2$ can be written as

$$\dot{V}_2 = \dot{V}_1 + \frac{\mathbf{e}_2^T}{k_1}\left(k_1\dot{\boldsymbol{\sigma}}(\mathbf{e_1}) + \boldsymbol{\delta} - \boldsymbol{\Gamma}\boldsymbol{\mu}\right). \tag{16}$$

Notice that $\boldsymbol{\Gamma}$ is invertible provided that $d_x \neq 0$. To obtain the convergence of the errors in the presence of constant perturbations, the integral state $\boldsymbol{\xi}$ with time derivative given by

$$\dot{\boldsymbol{\xi}} = \mathbf{e}_2 \tag{17}$$

is introduced. Consider a new candidate Lyapunov function given by

$$V_3 = V_2 + \frac{k_3}{2}\boldsymbol{\xi}^T\boldsymbol{\xi}. \tag{18}$$

The time derivative of V_3 can be written as

$$\dot{V}_3 = \dot{V}_1 + \frac{\mathbf{e}_2^T}{k_1}\left(k_1\dot{\boldsymbol{\sigma}}(\mathbf{e_1}) + \boldsymbol{\delta} + k_1k_3\boldsymbol{\xi} - \boldsymbol{\Gamma}\boldsymbol{\mu}\right). \tag{19}$$

At this point we can define a control law for $\boldsymbol{\mu}$ that renders $\dot{V}_3$ negative semi-definite and globally asymptotically stabilizes the origin of the error system. This result is stated formally in the following theorem.

Theorem 1: Consider the simplified vehicle model described by (3)-(6) and the error system with state given by $\mathbf{e}_1$, $\mathbf{e}_2$, and $\boldsymbol{\xi}$. The control law

$$\boldsymbol{\mu} = \Gamma^{-1}\left(\boldsymbol{\delta} + k_1\dot{\boldsymbol{\sigma}}(\mathbf{e_1}) + k_1^2k_2\mathbf{e}_2 + k_1k_3\boldsymbol{\xi}\right), \tag{20}$$

with $k_1 > 0$, $k_2 > \sqrt{2}$, and $k_3 > 0$, globally asymptotically stabilizes the origin of the error system.

Proof: Using the control law (20), the overall closed-loop system can be written as

$$\dot{\mathbf{e}}_1 = -S(r)\mathbf{e}_1 - k_1\boldsymbol{\sigma}(\mathbf{e_1})\boldsymbol{\sigma}(\mathbf{e}_1) + k_1\mathbf{e}_2, \tag{21}$$

$$\dot{\mathbf{e}}_2 = -k_1k_2\mathbf{e}_2 - k_3\boldsymbol{\xi}, \tag{22}$$

$$\dot{\boldsymbol{\xi}} = \mathbf{e}_2. \tag{23}$$

By noting that the dynamics of $\mathbf{e}_2$ and $\boldsymbol{\xi}$ do not depend on $\mathbf{e}_1$, we can immediately conclude that for positive gains k_1, k_2, and k_3, the origin of the subsystem (22)-(23) is globally asymptotically stable.

To analyze the stability of (21)-(23), note that substituting (20) in (19) yields

$$\begin{aligned} \dot{V}_3 &= -k_1\mathbf{e}_1^T\boldsymbol{\sigma}(\mathbf{e_1}) + k_1\mathbf{e}_1^T\mathbf{e}_2 - k_1k_2\mathbf{e}_2^T\mathbf{e}_2 \\ &\leq -\tfrac{\sqrt{2}}{2}k_1\|\mathbf{e}_1\|\|\boldsymbol{\sigma}(\mathbf{e_1})\| + k_1\|\mathbf{e}_1\|\|\mathbf{e}_2\| - k_1k_2\|\mathbf{e}_2\|^2 \end{aligned}$$

which is negative semi-definite whenever $\|\mathbf{e}_2\| \leq \frac{\sqrt{2}}{2}\|\boldsymbol{\sigma}(\mathbf{e_1})\|$ or $\|\mathbf{e}_1\| \leq k_2\|\mathbf{e}_2\|$. If $k_2 > \sqrt{2}$ and $\|\mathbf{e}_2\| \leq K$, then at least one of these conditions is satisfied. Since there exists a finite time T, such that for $t > T$ we have $\|\mathbf{e}_2(t)\| \leq K$, then $\dot{V}_3$ will become negative semi-definite in finite time and we can apply LaSalle's Invariance Principle to conclude that the origin is globally asymptotically stable. ■

C. Internal Dynamics Analysis

Having a control law that stabilizes the error system may not be sufficient to guarantee that the whole state of the vehicle is stabilized. In fact, for a given leader's position and a given $\mathbf{d}$, there are infinite solutions that satisfy (2), which indicates the existence of an internal dynamics, whose stability needs to be analyzed.

In this section, we show that the behavior of the zero-dynamics depends heavily on the x-component of the distance vector d_x, which should be judiciously chosen to guarantee the generation of adequate formation trajectories. Towards that end, consider the limit condition when the errors have converged to zero. In that situation, we can write

$$\begin{bmatrix} u \\ \dot{\theta} \end{bmatrix} = \mathbf{\Gamma}^{-1}\mathcal{R}^T \dot{\mathbf{p}}_L. \tag{24}$$

Let $\dot{\mathbf{p}}_L$ be given by

$$\dot{\mathbf{p}}_L = V_L \begin{bmatrix} \cos\theta_L \\ \sin\theta_L \end{bmatrix}, \tag{25}$$

with V_L and θ_L continuous functions representing the norm and direction of movement of the leader, respectively. Using these definitions, equation (24) can be rearranged into the form

$$\begin{bmatrix} u \\ \dot{\theta} \end{bmatrix} = \begin{bmatrix} V_L \cos(\theta_L - \theta) + \dfrac{V_L d_y}{d_x} \sin(\theta_L - \theta) \\ \dfrac{V_L}{d_x} \sin(\theta_L - \theta) \end{bmatrix}. \tag{26}$$

Applying the change of variables $\theta_d = \theta - \theta_L$, the zero-dynamics can be written as

$$\dot{\theta}_d = -\frac{V_L}{d_x}(\sin\theta_d + d_x\kappa_L), \tag{27}$$

where $\kappa_L = \omega_L/V_L$ is the curvature of the leader's path. It is worth noting that (27) does not depend on d_y. The analysis that follows is divided in two cases: a) trajectories with $\dot{\kappa}_L = 0$; and b) trajectories with $\dot{\kappa}_L \neq 0$.

For $\dot{\kappa}_L = 0$: Trajectories with $\dot{\kappa}_L = 0$ can be either a circumference ($\kappa_L \neq 0$), or a straight line ($\kappa_L = 0$). To analyze the stability of (27) for this type of trajectories, consider the candidate Lyapunov function

$$V_\theta = \frac{1}{2}(\sin\theta_d + d_x\kappa_L)^2, \tag{28}$$

whose time derivative is given by

$$\dot{V}_\theta = -2\frac{V_L}{d_x}\cos\theta_d\, V_\psi. \tag{29}$$

For simplicity, consider the case when $d_x > 0$ (a similar reasoning can be applied when $d_x < 0$). From (29), it follows that $\dot{V}_\theta$ is zero for $\theta_d = \pm\pi/2$ and for $\sin\theta_d = -d_x\kappa_L$, and negative definite whenever $\cos\theta_d > 0$. Analyzing (29), it can be shown that, if $|d_x\kappa_L| \leq 1$ then $\theta_d = -\arcsin(d_x\kappa_L)$ is an asymptotically stable equilibrium point, whereas $\theta_d = \pi - \arcsin(d_x\kappa_L)$ is unstable. Also, if $|d_x\kappa_L| > 1$ then $\lim_{t\to+\infty}|\theta_d| = +\infty$. From (26), it follows immediately that $|\dot{\theta}| \leq |\frac{V_L}{d_x}|$ and therefore $|\dot{\theta}| < |\dot{\theta}_L|$, meaning that the follower can never reach the angular velocity of the leader and the angular distance θ_d diverges. Notice however, that the condition $|d_x\kappa_L| \leq 1$ imposes no constraint on the curvature of the follower, since we can use d_y to select an arbitrary curvature.

For $\dot{\kappa}_L \neq 0$: When the trajectory being tracked has a time-varying curvature, the analysis is more involved and asymptotic stability for the general case is difficult to assess. Nevertheless, it is possible to prove the boundedness of θ_d, provided that $|d_x\kappa_L| < 1$, for all time. The following proposition is provided for $d_x > 0$. A similar reasoning can be applied for $d_x < 0$.

Lemma 2: Assume that $d_x > 0$ and $|d_x\kappa_L(t)| < \varepsilon < 1$, for all $t \geq 0$. Let Ω_1 and Ω_2 denote the sets $\Omega_1 = \{\theta_d : |\sin\theta_d| \leq \varepsilon, \cos\theta_d > 0\}$ and $\Omega_2 = \Omega_1 \cup \{\theta_d : |\sin\theta_d| \geq \varepsilon\}$, respectively. Then $\theta_d(t)$ is bounded, Ω_1 and Ω_2 are positively invariant, and any solution starting in Ω_2 will enter Ω_1 in finite time.

Proof: Consider the Lyapunov function

$$W_\theta = 1 - \cos\theta_d. \tag{30}$$

Computing the time derivative of W_θ, it can be shown that

$$\dot{W}_\theta \leq -\frac{V_L}{d_x}|\sin\theta_d|\,(|\sin\theta_d| - \varepsilon),$$

which is negative definite for $|\sin\theta_d| \geq \varepsilon$. Hence, the sets Ω_1 and Ω_2 are positively invariant and any solution starting in Ω_2 will enter Ω_1 in finite time. Solutions starting outside the set Ω_2 cannot grow unbounded, since to do so they would have to enter Ω_2, in which case the above applies. Thus, provided that $\varepsilon < 1$, θ_d is bounded irrespective of its initially value. ■

Above certain values of $|d_x\kappa_L|$, inversions in the directions of motion of the virtual followers may occur. Such behavior can affect the performance of the real vehicles tracking the generated trajectories and thus it is of interest to avoid it.

Rewriting the first part of (26) as

$$u\frac{d_x}{V_L} = d_x\cos\theta_d - d_y\sin\theta_d,$$

and assuming once again that $d_x > 0$, it can be shown that u will remain positive as long as

$$d_y\sin\theta_d > d_x\cos\theta_d$$

holds. Combining this condition with Lemma 2, we can obtain a bound for the initial value of the angular distance $\theta_d(0)$, which guarantees that no inversion will occur. More specifically, if

$$\arcsin|d_x\kappa_L(t)| < \text{atan2}(d_x, |d_y|) \tag{31}$$

$u(0) > 0$, and $\theta_d(0) \in \Omega_1$, then $u(t) > 0$, for all $t > 0$.

Lemma 2 shows that if a bound on the curvature of the leader's path κ_L is known, d_x can be chosen so as to guarantee that the angular distance between the leader and follower given by θ_d also remains within known bounds. This boundedness property (which is a direct consequence of the kinematic constraints imposed on the motion of the virtual follower) together with the stability in position guarantee that the generated trajectory is "well-behaved" and simultaneously that it is more complex than a simple offset version

of the leader's trajectory. The simulation results presented in the following section illustrate the type of trajectories that can be generated without the need to explicitly compute the leader's path parameters.

D. Simulation Results

This section presents the results of a simulation where two virtual vehicles were set to follow a leader describing a trajectory given by

$$\mathbf{p}_L(\gamma) = \begin{bmatrix} \frac{3}{2}\frac{\sin(\gamma/3)}{1+\sin^2(\gamma/3)} \\ \frac{3}{4}\frac{\sin(2\gamma/3)}{1+\sin^2(\gamma/3)} \end{bmatrix} \tag{32}$$

where $\dot{\gamma} = \sqrt{1+\sin^2\gamma}$, in order to produce a constant linear speed.

The desired distance for follower 1 is set to $\mathbf{d}_1 = [0.35\ 0.35]^T$ and its initial state to $\mathbf{p}_{F1}(0) = [-1\ 2]^T$, $u_{F1}(0) = 0.5$, $\omega_{F1}(0) = -0.5$, $\theta_{F1}(0) = 3\pi/2$. For follower 2, we select $\mathbf{d}_2 = [0.35\ -0.35]^T$ and set the initial state to $\mathbf{p}_{F2}(0) = [2\ 2]^T$, $u_{F2}(0) = 0$, $\omega_{F2}(0) = 0.5$, $\theta_{F2}(0) = \pi/2$. The controller parameters are $k_1 = 0.3$, $k_2 = 1.1$, $k_3 = 0.17$, and $p_{\max} = 5$.

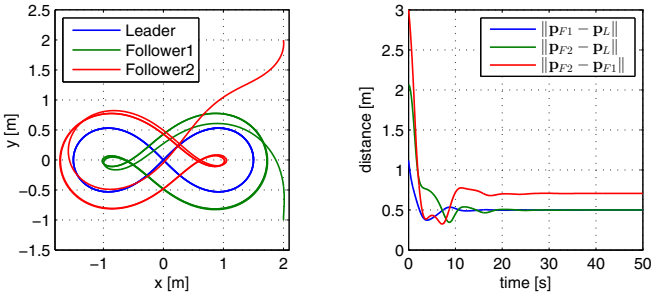

(a) Position (b) Distance between virtual vehicles

Fig. 1. Position and distance between vehicles during a simulation.

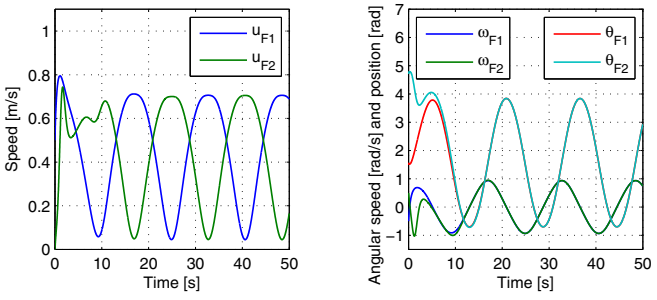

(a) Speed (b) Angular speed and position

Fig. 2. Virtual followers states.

Although the trajectories of both followers are different, see Fig. 1(a), their angular velocities and angular positions converge to the same values, as shown in Fig. 2(b). This is in accordance with the analysis made in Section II-C, as these variables do not depend on d_y, the only parameter that is different between followers in this simulation.

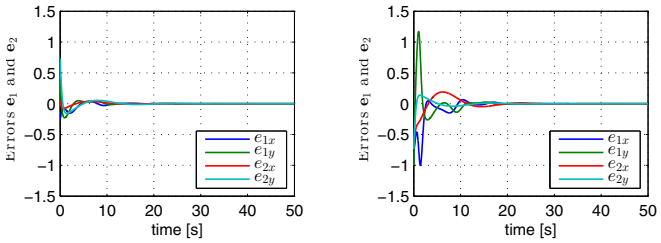

(a) Virtual follower 1 (b) Virtual follower 2

Fig. 3. Errors during a simulation.

Figure 1(b) indicates that the distance between followers and between these and the leader converge to fixed values. The latter is a direct implication of the asymptotic stability of the origin of the error system, see Fig. 3. The former results from the fact that d_x is equal for both followers, and thus their zero-dynamics are identical. The limit to which the distance between followers converges is equal to the sum of the leader-follower distances, in this case $0.35 + 0.35 = 0.7$m. These results indicate that, a formation where all the followers have the same value of d_x is asymptotically a rigid formation.

E. Three-dimensional trajectories

So far only two-dimensional motion has been considered. However, to generate trajectories for quadrotors it is necessary to consider three-dimensional motion. Instead of deriving a law for the entire state space, a separate control law is designed to drive the vertical coordinate of the virtual follower to a desired distance to the leader. Consider that the desired vectorial distance $\mathbf{d}$ is extended to include a third component d_z and let e_z be the vertical position error given by

$$e_z = p_{Lz} - p_{Fz} - d_z \tag{33}$$

A simple control law that stabilizes e_z is given by

$$\ddot{p}_{Fz} = \sigma_K(\ddot{p}_{Lz}) + \sigma_K(k_{z1}e_z + k_{z2}\dot{e}_z), \tag{34}$$

where

$$\sigma_K(x) = \begin{cases} x & \text{if } |x| \le K \\ \text{sign}(x)K & \text{if } |x| > K \end{cases} \tag{35}$$

This saturation is introduced to protect the followers from any unexpected acceleration of the leader. The control law asymptotically stabilizes e_z at the origin, provided that $|\ddot{p}_{Lz}| < K$ holds.

F. Planner initialization

As noted in Section II-C, inversions in the directions of movement of the virtual followers can affect the performance of the real vehicles tracking the trajectories. In order to prevent this behavior, the trajectory described by the leader and the desired configurations of the virtual followers have to satisfy (31). To comply with the bounds on the initial conditions, the virtual followers are initially placed with $\theta_d = 0$ and null errors, with respect to the reference trajectory of the leader, while the real vehicles are converging to their formation positions.

Until both the leader and follower vehicles approach the initial reference and virtual followers, respectively, the planner is kept turned off. Once that happens the planner

is turned on and the leader starts tracking the reference trajectory. The choice to initially place the virtual followers with respect to the reference trajectory of the leader allows for faster formation initialization, and guarantees that, when the planner is finally started, the actual values of the angles θ_d are within the computed bounds.

The tracking is triggered when the components of the position error of each vehicle satisfy the condition $e_i = \|\mathbf{p}_{Fi} - \mathbf{p}_{vFi}(0)\| < e_{\max}$, i.e.,

$$trigger = (e_L < e_{\max}) \wedge (e_1 < e_{\max}) \wedge \cdots \wedge (e_n < e_{\max}) \quad (36)$$

where $e_{\max}$ is a configurable parameter that defines the threshold used to start the tracking.

III. Experimental Test

This section presents the results of an experimental test carried out at the Sensor-Based Cooperative Robotics Research Laboratory – SCORE Lab of the Faculty of Science and Technology of the University of Macau.

Three quadrotors Blade mQX [10] were used in the experiment. These vehicles weigh 78g, have a length of 353mm and are actuated in terms of thrust and angular velocity. They are designed to be human piloted with remote controls. However, it was possible to identify the radio chip inside the remote control and connect the serial interface of the RF module to a computer serial port. A VICON [11] system, composed of 12 high speed cameras and a set of markers attached to the quadrotors, was used to capture the motion and attitude of the vehicles at 50Hz.

Two computers were used to perform the flight tests. One running the VICON software and a Simulink model, which generates the command signals sent to the other computer through Ethernet, and a second one that sends them through serial port to the RF module at 44Hz. The decision to separate control and communications was made to avoid jitter in the transmission of the serial-port signals to the RF module. A block diagram of the overall architecture is presented in Fig. 4.

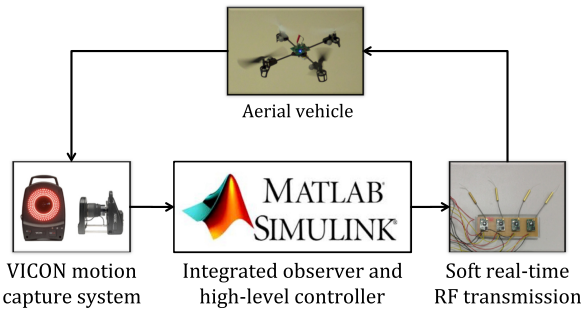

Fig. 4. System architecture.

The Simulink model used contains the trajectory planner developed and three quadrotor controllers. This controller is an adaptation of the one presented in [12], with actuation in thrust and angular velocity rather than thrust and torque, given that the Blade mQX quadrotor is actuated in thrust and angular velocity. An inner-loop controller is responsible for tracking the angular velocity commands.

The VICON system outputs a pre-filtered position of the vehicle and using the Euler approximation, it is possible to obtain a clean estimate of the velocity. However, the Euler approximation applied to the velocity estimates is highly contaminated by noise, degrading the quality of the estimated acceleration signals. To overcome this problem, a low-pass filter was applied to the measurements. Using experimental data taken from earlier tests performed with a quadrotor, it was possible to test the performance of various filters, with different dimensions. The best trade-off between responsiveness and smoothing was achieved with a moving average filter with 100 coefficients, which introduces a delay of approximately 1s.

A. Results

In this experimental evaluation the leader is tracking a trajectory given by (32) at a constant height of $h = -1.6$m. The trajectory is rotated by $\pi/4$ rad counter-clockwise and translated by $[0\ 0.5\ 0]$ m, to take full advantage of the space available in the laboratory (see Figure 5).

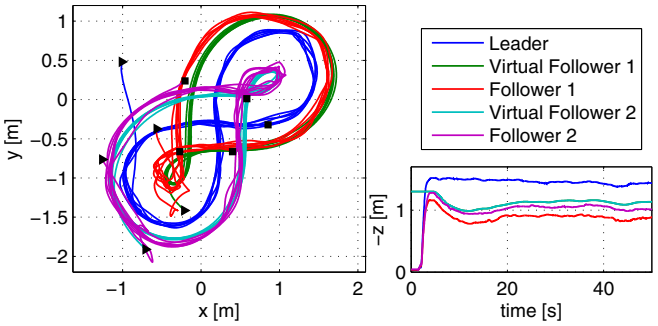

Fig. 5. Leader trajectory (blue), generated trajectories (green and cyan), and follower trajectories (red and magenta).

At the beginning of the test the quadrotors were at rest. The initial positions of the leader, follower 1, and follower 2 were $\mathbf{p}_L(0) = [-1\ 0.48\ 0]^T$m, $\mathbf{p}_{F1}(0) = [-0.57\ -0.37\ 0]^T$m, and $\mathbf{p}_{F2}(0) = [-1.26\ -0.77\ 0]^T$m, respectively. The distance vectors $\mathbf{d}$ for each follower were $\mathbf{d}_1 = [0.35\ 0.35\ -0.3]^T$m and $\mathbf{d}_2 = [0.35\ -0.35\ -0.3]^T$m. The control gains and saturation parameters used for the planner were $k_1 = 0.3$, $k_2 = 1.1$, $k_3 = 0.17$, $k_{z1} = 0.2$, $k_{z2} = 1$, and $p_{\max} = 5$.

Figure 5 shows in separate plots the x-y plane view and the time evolution of the z-coordinate for the trajectory described by the leader, the reference trajectories described by the virtual vehicles, and the actual trajectories described by the follower vehicles. The triangles indicate the initial positions of the vehicles and the squares the positions at the end of the simulation. Figure 5 shows that the planner is able to generate adequate reference trajectories and the quadrotors are able to track them, using the trajectory tracking controller proposed.

The generated reference trajectories capture the essence of leader's motion, while neglecting the higher frequency perturbations. For example in the z-coordinate plot, the longer and slower variations found in the leader's height can also be found in the height of the virtual followers. The high-frequency variations in the leader's height are filtered and do not appear in the generated trajectories. This process results in smoother trajectories that can be adequately

tracked, as can be seen from the time evolution of velocities and trajectory tracking errors (see Figures 6 and 7).

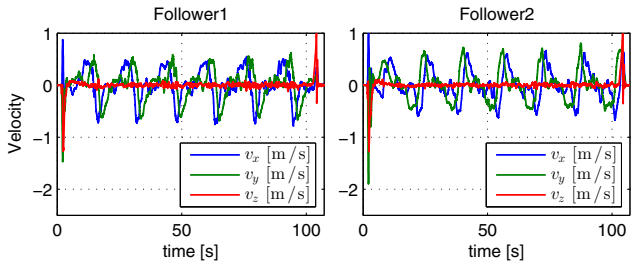

Fig. 6. Time evolution of velocities for both the followers.

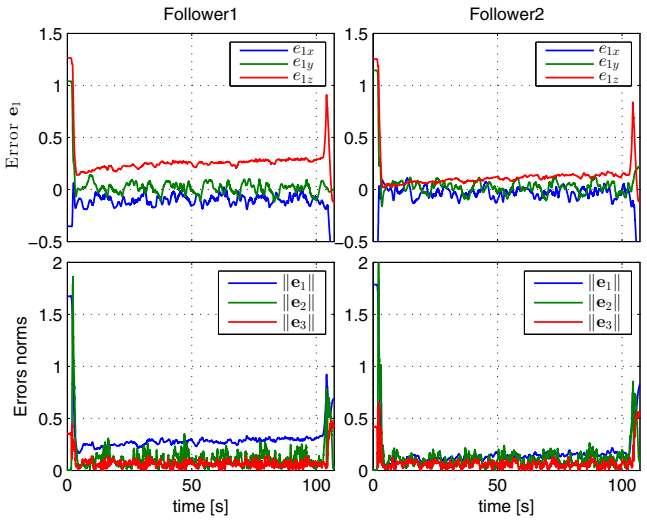

Fig. 7. Time evolution of the trajectory tracking errors for both followers.

Figure 8 shows the time evolution of the errors for the virtual vehicles, which exhibit an oscillatory behavior. This oscillation is a result of the trade-off that was found between mitigating the position error $\mathbf{e}_1$ and limiting the sensitiveness of the trajectories to the perturbations in leader's trajectory. It is possible to maintain the virtual errors close to the origin, but at the cost of degrading the trajectory tracking performance.

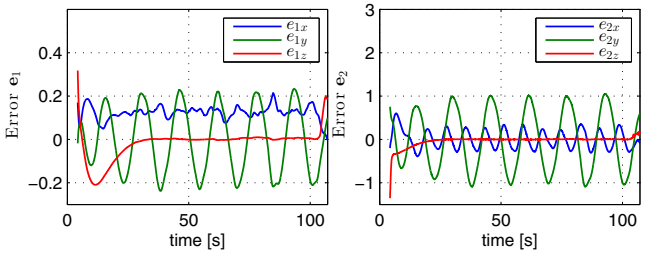

Fig. 8. Time evolution of the errors for both virtual followers.

IV. Conclusion

This paper presented a strategy for formation control of autonomous air vehicles. A leader-follower approach was adopted, which relies on a nonlinear control law to stabilize, at a predefined distance vector, the position of the leader in the body frame of a set of virtual followers. Global asymptotic stabilization of the leader-follower linear distance together with local boundedness of the leader-follower angular distances are guaranteed, provided that well-defined conditions relating the curvature of the leader's trajectory and the desired distances between vehicles are met.

Experimental tests were performed to demonstrate the applicability of the method to the task controlling quadrotors in formation, showing that the generated trajectories are easily tracked by the vehicles. In spite of the fact that only the leader's position was being measured, the computation of smoothed single and double differences allowed for an adequate generation and accurate tracking of formation trajectories.

Directions of future work include exploring other possibilities of virtual vehicle models, developing collision avoidance capabilities for the planner, and improving and optimizing the motion estimation.

References

[1] P. Ogren, E. Fiorelli, and N. E. Leonard, "Cooperative control of mobile sensor networks: Adaptive gradient climbing in a distributed environment," *IEEE Transactions on Automatic Control*, vol. 49, pp. 1292–1302, 2004.

[2] S. Waharte, N. Trigoni, and S. Julier, "Coordinated search with a swarm of uavs," in *Sensor, Mesh and Ad Hoc Communications and Networks Workshops, 2009. SECON Workshops '09. 6th Annual IEEE Communications Society Conference on*, pp. 1 –3, june 2009.

[3] N. Michael, J. Fink, and V. Kumar, "Cooperative manipulation and transportation with aerial robots," *Autonomous Robots*, vol. 30, pp. 73–86, january 2011.

[4] N. Leonard and E. Fiorelli, "Virtual leaders, artificial potentials and coordinated control of groups," in *Decision and Control, 2001. Proceedings of the 40th IEEE Conference on*, vol. 3, pp. 2968 –2973 vol.3, 2001.

[5] R. Olfati-Saber, "Flocking for multi-agent dynamic systems: algorithms and theory," *Automatic Control, IEEE Transactions on*, vol. 51, pp. 401 – 420, march 2006.

[6] E. Justh and P. Krishnaprasad, "Equilibria and steering laws for planar formations," *Systems and Control Letters*, vol. 52, no. 1, pp. 25 – 38, 2004.

[7] J. Guerrero and R. Lozano, "Flight formation of multiple mini rotorcraft based on nested saturations," in *Intelligent Robots and Systems (IROS), 2010 IEEE/RSJ International Conference on*, pp. 634 –639, October 2010.

[8] H. Tanner, G. Pappas, and V. Kumar, "Leader-to-formation stability," *IEEE Transactions on Robotics and Automation*, vol. 20, no. 3, pp. 443–455, 2004.

[9] M. Turpin, N. Michael, and V. Kumar, "Trajectory design and control for aggressive formation flight with quadrotors," *Autonomous Robots*, vol. 33, pp. 143–156, 2012.

[10] "Horizon hobby." `http://www.horizonhobby.com/`, October 2012.

[11] "Vicon system." `http://www.vicon.com/`, October 2012.

[12] D. Cabecinhas, R. Cunha, and C. Silvestre, "Rotorcraft path following control for extended flight envelope coverage," in *Decision and Control, 2009 held jointly with the 2009 28th Chinese Control Conference. CDC/CCC 2009. Proceedings of the 48th IEEE Conference on*, pp. 3460 –3465, dec. 2009.